



|                  |   |
|------------------|---|
| Title            | Regional interaction between myocardial sympathetic denervation, contractile dysfunction, and fibrosis in heart failure with preserved ejection fraction : 11C-hydroxyephedrine PET study |
| Author(s)        | Aikawa, Tadao; Naya, Masanao; Obara, Masahiko; Oyama-Manabe, Noriko; Manabe, Osamu; Magota, Keiichi; Ito, Yoichi M.; Katoh, Chietsugu; Tamaki, Nagara                                     |
| Citation         | European Journal of Nuclear Medicine and Molecular Imaging, 44(11), 1897-1905<br><a href="https://doi.org/10.1007/s00259-017-3760-y">https://doi.org/10.1007/s00259-017-3760-y</a>        |
| Issue Date       | 2017-10   |
| Doc URL          | <a href="http://hdl.handle.net/2115/71560">http://hdl.handle.net/2115/71560</a>   |
| Rights           | The final publication is available at <a href="http://link.springer.com">link.springer.com</a>  |
| Type             | article (author version)  |
| File Information | HUSCAP_EJNM-D-17-00342_20170628.pdf   |



[Instructions for use](#)

**Regional interaction between myocardial sympathetic denervation, contractile dysfunction, and fibrosis in heart failure with preserved ejection fraction: <sup>11</sup>C-hydroxyephedrine PET study**

Tadao Aikawa, MD;<sup>1</sup> Masanao Naya, MD, PhD;<sup>1\*</sup> Masahiko Obara, MD, PhD;<sup>1</sup> Noriko Oyama-Manabe, MD, PhD;<sup>2</sup> Osamu Manabe, MD, PhD;<sup>3</sup> Keiichi Magota, PhD;<sup>4</sup> Yoichi M. Ito, PhD;<sup>5</sup> Chietsugu Katoh, MD, PhD;<sup>6</sup> and Nagara Tamaki, MD, PhD<sup>7</sup>

<sup>1</sup>Department of Cardiovascular Medicine, Faculty of Medicine and Graduate School of Medicine, Hokkaido University, Kita-15, Nishi-7, Kita-ku, Sapporo 060-8638, Japan

<sup>2</sup>Department of Diagnostic and Interventional Radiology, Hokkaido University Hospital, Kita-14, Nishi-5, Kita-ku, Sapporo 060-8648, Japan

<sup>3</sup>Department of Nuclear Medicine, Faculty of Medicine and Graduate School of Medicine, Hokkaido University, Kita-15, Nishi-7, Kita-ku, Sapporo 060-8638, Japan

<sup>4</sup>Division of Medical Imaging and Technology, Hokkaido University Hospital, Kita-14, Nishi-5, Kita-ku, Sapporo 060-8648, Japan

<sup>5</sup>Department of Biostatistics, Faculty of Medicine and Graduate School of Medicine, Hokkaido University, Kita-15, Nishi-7, Kita-ku, Sapporo 060-8638, Japan

<sup>6</sup>Department of Biomedical Science and Engineering, Faculty of Health Sciences, Hokkaido University, Kita-15, Nishi-7, Kita-ku, Sapporo 060-8638, Japan

<sup>7</sup>Department of Radiology, Kyoto Prefectural University of Medicine, Kajii-cho, Kawaramachi-Hirokoji, Kamigyo-ku, Kyoto 602-8566, Japan

\*Correspondence to: Masanao Naya

Tel.: +81-11-706-6973

Fax: +81-11-706-7874

E-mail: [naya@med.hokudai.ac.jp](mailto:naya@med.hokudai.ac.jp)

Word count: 5,584

ORCID No.: Tadao Aikawa (0000000217860176)

**Funding Sources:** Grant-in-aid for scientific research (JP24591742) from the Ministry of Education, Culture, Sports, Science, and Technology (M.N.).

**Abstract**

*Purpose:* This investigation aimed to identify significant predictors of regional sympathetic denervation quantified by  $^{11}\text{C}$ -hydroxyephedrine (HED) positron emission tomography (PET) in patients with heart failure with preserved left ventricular ejection fraction (HFpEF).

*Methods:* Thirty-four patients ( $63 \pm 15$  years, 23 male) with HFpEF (left ventricular ejection fraction  $\geq 40\%$ ) and 11 age-matched volunteers without heart failure were included. Cardiac magnetic resonance imaging was performed to measure left ventricular size, function, and the extent of myocardial late gadolinium enhancement (LGE).  $^{11}\text{C}$ -HED PET was performed to quantify myocardial sympathetic innervation expressed as  $^{11}\text{C}$ -HED retention index (RI [%/min]). To identify predictors of regional  $^{11}\text{C}$ -HED RI in HFpEF patients, we proposed a multivariate mixed-effects model for repeated measures over segments with an unstructured covariance matrix.

*Results:* Global  $^{11}\text{C}$ -HED RI was significantly lower and more heterogeneous in HFpEF patients versus volunteers ( $P < 0.01$  for all). Regional  $^{11}\text{C}$ -HED RI correlated positively with systolic wall thickening ( $r = 0.42$ ,  $P < 0.001$ ) and negatively with the extent of LGE ( $r = -0.43$ ,  $P < 0.001$ ). Segments with large extent of LGE in HFpEF patients had the lowest regional  $^{11}\text{C}$ -HED RI among all segments ( $P < 0.001$  for post hoc tests). Multivariate analysis demonstrated that systolic wall thickening and the extent of LGE were significant predictors of regional  $^{11}\text{C}$ -HED RI in HFpEF patients (both  $P \leq 0.001$ ).

*Conclusion:* Regional sympathetic denervation was associated with contractile dysfunction and fibrotic burden in HFpEF patients, suggesting that regional sympathetic denervation may provide an integrated measure of myocardial damage in HFpEF.

**Keywords:** heart failure with preserved ejection fraction,  $^{11}\text{C}$ -hydroxyephedrine, regional sympathetic denervation, contractile dysfunction, myocardial fibrosis

## Introduction

Myocardial sympathetic denervation has been recognized as an indicator of poor prognosis in patients with heart failure [1, 2]. Regional sympathetic denervation in particular was found to be a significant predictor of sudden cardiac death in patients with ischemic cardiomyopathy independent of infarct size [3]. An animal study using a porcine infarction model showed a stepwise decrease in myocardial sympathetic innervation and systolic wall thickening between normal, adjacent, and infarcted myocardium [4]. Regional denervated myocardium has also been observed in patients with idiopathic dilated cardiomyopathy [5-7] and hypertrophic cardiomyopathy [8-10]. These findings suggest that regional sympathetic denervation may reflect functional and pathological alterations in both ischemic and nonischemic cardiomyopathy. Most previous studies have focused on myocardial sympathetic denervation in patients with heart failure with left ventricular (LV) ejection fraction < 40% [1-3, 5-7], while the implication of regional sympathetic denervation in those with LV ejection fraction  $\geq$  40%, which has been termed heart failure with preserved ejection fraction (HFpEF), has not been well investigated.

HFpEF is a common form of heart failure and is functionally characterized by diastolic dysfunction accompanying myocardial fibrosis [11, 12]. Recently, we demonstrated that myocardial sympathetic denervation, as measured by  $^{11}\text{C}$ -hydroxyephedrine ( $^{11}\text{C}$ -HED) positron emission tomography (PET), in patients with HFpEF was related to the severity of diastolic dysfunction independently of LV ejection fraction [13]. A detailed understanding of the regional sympathetic denervation in patients with HFpEF may be useful for risk stratification or monitoring because myocardial sympathetic denervation may reflect the pathophysiologic

process of HFpEF. Cardiac magnetic resonance (CMR) allows noninvasive assessment of contractile function and fibrotic changes in various cardiomyopathies [14-16]. Thus, we aimed to identify the predictors of regional sympathetic denervation in patients with HFpEF by functional and morphological tissue characterization using  $^{11}\text{C}$ -HED PET and CMR.

## Materials and methods

### Study Population

We studied 34 patients with HFpEF at Hokkaido University Hospital between November 2012 and November 2015. HFpEF was diagnosed in a patient when all of the following criteria were met: chronic congestive heart failure, diagnosed based on the Framingham Heart Study criteria [17], presence of LV ejection fraction  $\geq 40\%$ , based on two-dimensional echocardiography; and having a history of hospital admission for cardiac reasons. HFpEF patients were divided into those with coronary artery disease (CAD,  $n = 11$ ) and those without CAD (non-CAD,  $n = 23$ ), defined by  $\geq 70\%$  narrowing of a major epicardial coronary artery, detected on performing invasive coronary angiography; history of myocardial infarction; or evidence of ischemia or infarction, detected on performing stress myocardial perfusion imaging [18]. All participants were recruited as part of a previous study [13]. Exclusion criteria were severe left-sided valvular heart disease on echocardiography, contraindications to cardiac magnetic resonance (such as metallic implants and claustrophobia), and estimated glomerular filtration rate  $< 30 \text{ mL}\cdot\text{min}^{-1}\cdot 1.73\text{m}^2$ . Eleven age-matched control participants with normal LV ejection fraction without valvular heart disease and no cardiovascular disease were also studied. All participants underwent CMR and  $^{11}\text{C}$ -HED PET within 1 month (median interval, 3 days; interquartile range, 0–7 days), and no clinical events occurred between the two tests. All patients were prospectively followed up by their physician, or via telephone interviews to assess adverse events, such as acute decompensated heart failure requiring hospitalization, life-threatening ventricular arrhythmias, and all-cause death. This study was approved by the ethics committee of Hokkaido University Hospital (IRB 012-0098) and was registered with the

University Hospital Medical Information Network clinical trials registry (UMIN000009386). All participants provided written informed consent.

### **CMR Protocol**

CMR was performed using a 1.5-T whole-body scanner (Achieva, Philips Medical Systems, Best, The Netherlands) with a 5-channel phased-array cardiac coil ( $n = 13$ ) or a 3-T whole-body scanner (Achieva TX, Philips Medical Systems) with a 32-channel phased-array receiver torso-cardiac coil ( $n = 32$ ) in accordance with standardized CMR protocols [19], as described elsewhere [20-22]. In brief, after localization of the heart, a series of LV short-axis cine images from base to apex were obtained using a retrospectively electrocardiogram-gated, balanced steady-state free precession pulse sequence during repeated breath-holds. Late gadolinium enhancement (LGE) images at matching cine-image slice locations were obtained 10–15 min after administration of 0.1 mmol/kg of Gd-DTPA using an inversion-recovery prepared, 3-dimensional fast field echo pulse sequence.

### **CMR Image Analysis**

CMR image analysis was performed using commercially available software (Ziostation2 Ziosoft Inc., Tokyo, Japan). LV volumes, ejection fraction, mass, and wall thickness were measured by semi-automatically outlining endocardial and epicardial borders of the myocardium on the short-axis cine images. Regional systolic wall thickening (%) was calculated as follows:  $([\text{end-diastolic wall thickness} - \text{end-systolic wall thickness}]/\text{end-}$

diastolic wall thickness)  $\times$  100%. The extent of hyperenhanced myocardium on LGE images was quantified as the percentage area of hyperenhanced myocardium using a 5-standard deviation threshold above the mean of remote myocardium [22, 23]. The LV myocardium was automatically divided into 16 segments of the American Heart Association 17-segment model, excluding the apex segment.

### **<sup>11</sup>C-HED PET Protocol**

<sup>11</sup>C-HED PET was performed using a whole-body PET/CT scanner (Biograph 64 TruePoint, Siemens Japan, Tokyo, Japan). Participants were instructed to fast for at least 4 hours prior to the scan, and to avoid caffeine- and methylxanthine-containing substances for at least 24 hours prior to the scan. <sup>11</sup>C-HED PET scanning was performed as described previously [13]. In brief, after a low-dose CT scan for attenuation and scatter correction, a bolus of 185 MBq of <sup>11</sup>C-HED was injected simultaneously with the start of a 40-min list-mode acquisition. PET images were reconstructed into 21 frames (9  $\times$  10, 3  $\times$  30, 2  $\times$  60, and 7  $\times$  300 s) using filtered back-projection with 10-mm full width at half maximum Gaussian postsMOOTHING, a matrix size of 128  $\times$  128, and a voxel size of 3.6  $\times$  3.6  $\times$  2.0 mm<sup>3</sup>.

### **PET Image Analysis**

PET image analysis was performed using in-house developed software. Short-axis images in the last frame of the dynamic scan were used to define a region of interest in the left ventricle, which was semi-automatically divided into the 17 segments based on the American Heart Association recommendation. Image-derived input

functions were obtained from a manually placed region of interest at the basal LV cavity of valve plane.  $^{11}\text{C}$ -HED retention index (RI [%/min]) as a measure of myocardial sympathetic innervation was calculated as the mean myocardial activity in the last frame (30 to 40 min) divided by the integral of the arterial input function [5, 7, 13]. The coefficient of variation of regional  $^{11}\text{C}$ -HED RI among the 17 segments (CVRI) was also calculated as a measure of heterogeneity in myocardial  $^{11}\text{C}$ -HED uptake [13]. A segment was considered to have a denervation-scar mismatch if the segment had no LGE (< 1% of the segment) and regional  $^{11}\text{C}$ -HED RI below the 2.5th percentile of the control group range (< 8.3 %/min). The mismatch size was expressed as %LV.

### **Statistical Analysis**

All statistical analyses were performed using JMP Pro 12.0.1 (SAS Institute Inc., Cary, North Carolina). Continuous variables are presented as median and interquartile range. Categorical variables are presented as absolute numbers and percentages. Significance of difference between groups was evaluated using the Kruskal–Wallis test followed by the Steel–Dwass test for multiple comparisons. Correlation between two variables was evaluated by performing linear regression analysis. Difference in LV ejection fraction measurements between those obtained using two-dimensional echocardiography and volumetric CMR were compared using the Wilcoxon signed-rank test. To assess the interaction between regional sympathetic denervation, systolic wall thickening, the extent of LGE, and LV end-diastolic wall thickness in patients with HFpEF on a per-segment basis, a multivariate analysis was performed using a mixed-effects model for repeated measures of the 16 segments per-patient, adjusting for age, sex, body mass index, past medical history (hypertension, diabetes,

hyperlipidaemia, and atrial fibrillation), the presence of CAD,  $\beta$ -blockers use, and intermediate LV ejection

fraction (< 50% based on CMR). An unstructured covariance matrix was used to account for correlation

between segments. A two-tailed  $P$  value of less than 0.05 was considered statistically significant.

## Results

### Clinical Characteristics

Clinical characteristics of participants are shown in Table 1. The non-CAD group included patients with diagnoses of hypertrophic cardiomyopathy ( $n = 7$ ), hypertensive heart disease ( $n = 4$ ), idiopathic dilated cardiomyopathy ( $n = 4$ ), cardiac sarcoidosis ( $n = 4$ ), cardiac amyloidosis ( $n = 2$ ), tachycardia-induced cardiomyopathy ( $n = 1$ ), and prior myocarditis ( $n = 1$ ). There was no significant difference in age among the control and HFpEF groups, although the CAD group was more likely to be male and more frequently treated with statins and antiplatelet agents. The majority of the two HFpEF groups (88%) had symptomatic heart failure (New York Heart Association class II–III). The levels of plasma B-type natriuretic peptide in the two HFpEF groups were significantly higher than those in the control group ( $P < 0.05$  for both).

### Per-Participant Analysis

Representative images are shown in Figure 1. Table 2 summarizes the PET and CMR imaging results. Overall, the two HFpEF groups had significantly larger LV volumes and masses, and a lower LV ejection fraction than the control group ( $P < 0.05$  for all). Although there were variations in LV measurements obtained using echocardiography and CMR, the comparison of LV ejection fractions between the two modalities showed good correlation ( $r = 0.90$ ,  $P < 0.001$ ), without significant differences (mean difference, 1.2%; 95% confidence interval,  $-1.0\%$  to  $3.5\%$ ;  $P = 0.38$ ). No participant in the control group had hyperenhanced myocardium on LGE images. Two patients with cardiac amyloidosis were excluded from further analysis because they showed diffuse

hyperenhancement on LGE images, the extent of which could not be measured. LV volume, mass, and the extent of LGE did not significantly differ between the two HFpEF groups. In the non-CAD group, patients with hypertrophic cardiomyopathy tended to have a higher LV mass (138.8 g [interquartile range: 114.1 to 212.5 g]) compared to those without (120.5 g [interquartile range: 93.9 to 135.6 g]). However, this difference was not statistically significant ( $P = 0.10$ ). Regarding the PET imaging results, the two HFpEF groups showed significantly lower global  $^{11}\text{C}$ -HED RI and larger CVRI than the control group ( $P < 0.01$  for all), whereas the global  $^{11}\text{C}$ -HED RI, CVRI, and denervation-scar mismatch size were not significantly different between the two HFpEF groups ( $P = 0.51$  and  $P = 0.96$ , respectively). On a participant basis, LV ejection fraction, volumes, mass, and the extent of LGE significantly correlated with global  $^{11}\text{C}$ -HED RI and CVRI ( $P < 0.05$  for all) (Table 3). The denervation-scar mismatch size did not significantly correlate with LV ejection fraction, volume, and mass ( $P =$  not significant for all).

### Per-Segment Analysis

Figure 2 shows scatter plots of interplay between regional  $^{11}\text{C}$ -HED RI and CMR imaging variables on a per-segment basis. Regional  $^{11}\text{C}$ -HED RI showed a significant positive correlation with systolic wall thickening ( $r = 0.42$ ,  $P < 0.001$ ) and a significant negative correlation with the extent of LGE ( $r = -0.43$ ,  $P < 0.001$ ). Despite excluding patients with LV ejection fractions  $< 40\%$ , based on CMR ( $n = 8$ ), these correlations were consistent ( $r = 0.35$  for systolic wall thickening vs. regional  $^{11}\text{C}$ -HED RI and  $r = -0.41$  for the extent of LGE vs. regional  $^{11}\text{C}$ -HED RI;  $P < 0.001$  for both). Regional  $^{11}\text{C}$ -HED RI did not show a simple linear relationship with LV end-

diastolic wall thickness. The distributions of regional  $^{11}\text{C}$ -HED RI in the control and HFpEF groups categorized by systolic wall thickening and the extent of LGE are shown in Figure 3. Segments with a large extent of LGE (> 10% of the segment) in HFpEF groups had the lowest  $^{11}\text{C}$ -HED RI among all segments of the population ( $P < 0.001$  for post hoc tests). The data showed a modest stepwise decrease in regional  $^{11}\text{C}$ -HED RI with decreasing systolic wall thickening and increasing the extent of LGE. The regional  $^{11}\text{C}$ -HED RI in segments with a small extent of LGE (1% to 10% of the segment) was comparable to that in segments with decreasing systolic wall thickening (< 75%) and no LGE ( $P = 1.00$ ).

### **Predictors of Regional Sympathetic Denervation in Cardiomyopathy**

Table 4 shows the results of the mixed-effects model exploring the interaction between regional  $^{11}\text{C}$ -HED RI, CMR imaging variables, and baseline characteristics in the two HFpEF groups on a per-segment basis. This analysis revealed that systolic wall thickening, the extent of LGE, and LV end-diastolic wall thickness were independently associated with regional  $^{11}\text{C}$ -HED RI ( $P \leq 0.001$  for all), whereas baseline characteristics, the presence of CAD, and intermediate LV ejection fraction (< 50%) were not significantly associated with regional  $^{11}\text{C}$ -HED RI.

### **Clinical Follow-up**

During the follow-up period (median, 21 months; range, 17 to 36 months), no patient died and appropriate implantable cardioverter-defibrillator discharge occurred in only 1 patient, in whom low global  $^{11}\text{C}$ -HED RI

(7.4 %/min) and large CVRI (17.7%) were observed. Two patients were admitted for acute decompensated heart

failure. The low event rate in the present study precluded meaningful interpretation of  $^{11}\text{C}$ -HED PET variables.

## Discussion

This study shows that myocardial sympathetic innervation in patients with HFpEF was more reduced and more heterogeneous than that in control participants. Denervation-scar mismatch was found in patients without CAD as well as those with CAD. On a per-segment basis, systolic wall thickening, the extent of LGE, and LV end-diastolic wall thickness were significant predictors of regional sympathetic denervation in patients with HFpEF, suggesting that regional sympathetic denervation may provide an integrated measure of myocardial damage in HFpEF.

Heterogenous reduction in myocardial sympathetic innervation in various cardiomyopathies was in line with previous studies [3, 5, 7-10]. Myocardial sympathetic denervation in CAD is observed in the infarct core and the surrounding border zone [3, 4, 24]. In contrast, denervated myocardium is located in the apex and inferior wall in patients with idiopathic dilated cardiomyopathy [5, 7] and in the hypertrophic wall in patients with hypertrophic cardiomyopathy [8], indicating that the heterogenous reduction may not be directly associated with myocardial ischemia in the failing heart.

On a per-segment basis, regional decrease in myocardial sympathetic innervation was found not only in the scar segments but also in the no-scar segments with contractile dysfunction. Furthermore, systolic wall thickening and the extent of myocardial scar were independently associated with regional sympathetic denervation in patients with HFpEF. These observations suggest that the autonomic nervous system may be involved in the early pathophysiologic changes in HFpEF. A previous study in patients with idiopathic dilated cardiomyopathy reported a significant correlation between regional  $^{11}\text{C}$ -HED RI and systolic wall thickening

[5]. Although regional sympathetic denervation in patients with HFpEF is expected to correlate with contractile dysfunction or myocardial scar, such data has been lacking so far. To our knowledge, this is the first study demonstrating a quantitative association between regional sympathetic denervation, contractile dysfunction, and myocardial scar in HFpEF due to various cardiomyopathies.

In contrast with a previous report in patients with hypertrophic cardiomyopathy [8], increase in LV wall thickness was associated with increase in regional sympathetic innervation on multivariate analysis. One of the possible reasons for this difference is the partial volume effect of  $^{11}\text{C}$ -HED, which can lead to overestimation of myocardial sympathetic innervation. To mitigate this, we included LV end-diastolic wall thickness in the multivariate mixed-effect models. In patients with hypertrophic cardiomyopathy, the hypertrophied region, typically in the interventricular septum, often has myocardial fibrosis (detected as LGE), which correlates with decreasing systolic wall thickening [16]. Therefore, both myocardial fibrosis and contractile dysfunction may affect regional sympathetic denervation in the hypertrophied region in patients with hypertrophic cardiomyopathy.

We have focused on regional decreases in myocardial  $^{11}\text{C}$ -HED uptake because the quantification of regional sympathetic denervation as a predictor of ventricular arrhythmias has been reported in clinical practice [3, 25]. Ischemic myocardium, which can be assessed by performing myocardial perfusion and metabolic imaging, is recognized as the most common cause of ventricular arrhythmias [26]. The extent of the denervated myocardium exceeds the infarction and indicates the ischemic area at risk [27], suggesting that they may assess a similar arrhythmogenic substrate. These findings, as well as our results, highlight a high sensitivity of

sympathetic innervation to various forms of myocardial damage.

Myocardial fibrosis is one of the significant substrates for ventricular arrhythmias. CMR allows noninvasive assessment of myocardial fibrosis; the presence and extent of LGE have been reported to predict adverse arrhythmic events in patients with cardiomyopathy [18]. Global and regional alterations in myocardial sympathetic innervation have also been described as a possible predictor of ventricular tachyarrhythmia [3, 25, 28, 29]. Recently, the Prediction of Arrhythmic Events with Positron Emission Tomography study of 204 patients with ischemic cardiomyopathy (mean LVEF,  $27\% \pm 9\%$ ) demonstrated that not infarct size or LV ejection fraction, but the extent of regional sympathetic denervation quantified using  $^{11}\text{C}$ -HED PET was an independent predictor of sudden cardiac death [3]. In contrast to CMR, cardiac sympathetic imaging can be applied to patients with implantable devices. Although the primary focus of this study is the cross-sectional comparison between regional sympathetic denervation and other variables, further research is required to clarify the clinical value of assessing regional sympathetic denervation in HFpEF.

The current study has several limitations. First, we did not perform stress myocardial perfusion imaging in the study participants. Myocardial perfusion may affect the sympathetic innervation; however, perfusion imaging is not necessarily required for the clinical assessment of HFpEF. Second, we did not evaluate the pattern of regional sympathetic denervation in patients with specific cardiomyopathies. However, multivariate analysis demonstrated the association between regional sympathetic denervation, contractile dysfunction, and myocardial scar independent of CAD. Third, this cross-sectional study cannot conclusively determine the cause-effect association between regional sympathetic denervation and other variables. Whether sympathetic

denervation primarily causes myocardial damage remains unclear.

## **Conclusion**

The present study demonstrates that regional sympathetic denervation was associated with contractile dysfunction and the extent of myocardial scar in patients with HFpEF, suggesting that regional sympathetic denervation may provide an integrated measure of myocardial damage in HFpEF. Further research is needed to assess the prognostic value of regional sympathetic denervation in HFpEF.

## **Compliance with ethical standards**

**Funding:** This work was supported by grant-in-aid for scientific research (grant no. JP24591742) from the Ministry of Education, Culture, Sports, Science, and Technology (M.N.).

**Conflicts of interest:** The authors declare that they have no conflict of interest.

**Ethical approval:** All procedures performed in studies involving human participants were in accordance with the ethical standards of the institutional and/or national research committee and with the 1964 Helsinki declaration and its later amendments or comparable ethical standards.

**Informed consent:** Informed consent was obtained from all individual participants included in the study.

## References

1. Jacobson AF, Senior R, Cerqueira MD, Wong ND, Thomas GS, Lopez VA, et al. Myocardial iodine-123 meta-iodobenzylguanidine imaging and cardiac events in heart failure. Results of the prospective ADMIRE-HF (AdreView Myocardial Imaging for Risk Evaluation in Heart Failure) study. *J Am Coll Cardiol.* 2010;55:2212-21.
2. Verberne HJ, Brewster LM, Somsen GA, van Eck-Smit BL. Prognostic value of myocardial <sup>123</sup>I-metaiodobenzylguanidine (MIBG) parameters in patients with heart failure: a systematic review. *Eur Heart J.* 2008;29:1147-59.
3. Fallavollita JA, Heavey BM, Luisi AJ, Jr., Michalek SM, Baldwa S, Mashtare TL, Jr., et al. Regional myocardial sympathetic denervation predicts the risk of sudden cardiac arrest in ischemic cardiomyopathy. *J Am Coll Cardiol.* 2014;63:141-9.
4. Lautamaki R, Sasano T, Higuchi T, Nekolla SG, Lardo AC, Holt DP, et al. Multiparametric molecular imaging provides mechanistic insights into sympathetic innervation impairment in the viable infarct border zone. *J Nucl Med.* 2015;56:457-63.
5. Bengel FM, Permanetter B, Ungerer M, Nekolla SG, Schwaiger M. Relationship between altered sympathetic innervation, oxidative metabolism and contractile function in the cardiomyopathic human heart; a non-invasive study using positron emission tomography. *Eur Heart J.* 2001;22:1594-600.
6. Henderson EB, Kahn JK, Corbett JR, Jansen DE, Pippin JJ, Kulkarni P, et al. Abnormal I-123 metaiodobenzylguanidine myocardial washout and distribution may reflect myocardial adrenergic derangement in patients with congestive cardiomyopathy. *Circulation.* 1988;78:1192-9.
7. Hartmann F, Ziegler S, Nekolla S, Hadamitzky M, Seyfarth M, Richardt G, et al. Regional patterns of myocardial sympathetic denervation in dilated cardiomyopathy: an analysis using carbon-11 hydroxyephedrine and positron emission tomography. *Heart.* 1999;81:262-70.
8. Li ST, Tack CJ, Fananapazir L, Goldstein DS. Myocardial perfusion and sympathetic innervation in patients with hypertrophic cardiomyopathy. *J Am Coll Cardiol.* 2000;35:1867-73.
9. Shimizu M, Ino H, Yamaguchi M, Terai H, Hayashi K, Nakajima K, et al. Heterogeneity of cardiac sympathetic nerve activity and systolic dysfunction in patients with hypertrophic cardiomyopathy. *J Nucl Med.* 2002;43:15-20.
10. Terai H, Shimizu M, Ino H, Yamaguchi M, Uchiyama K, Oe K, et al. Changes in cardiac sympathetic nerve innervation and activity in pathophysiologic transition from typical to end-stage hypertrophic cardiomyopathy. *J Nucl Med.* 2003;44:1612-7.
11. Redfield MM. Heart failure with preserved ejection fraction. *N Engl J Med.* 2016;375:1868-77.
12. Rommel KP, von Roeder M, Latuscynski K, Oberueck C, Blazek S, Fengler K, et al. Extracellular volume fraction for characterization of patients with heart failure and preserved ejection fraction. *J Am Coll Cardiol.* 2016;67:1815-25.
13. Aikawa T, Naya M, Obara M, Manabe O, Tomiyama Y, Magota K, et al. Impaired myocardial sympathetic innervation is associated with diastolic dysfunction in heart failure with preserved ejection fraction: <sup>11</sup>C-hydroxyephedrine PET study. *J Nucl Med.* 2017;58:784-90.

14. Mahrholdt H, Wagner A, Parker M, Regenfus M, Fieno DS, Bonow RO, et al. Relationship of contractile function to transmural extent of infarction in patients with chronic coronary artery disease. *J Am Coll Cardiol.* 2003;42:505-12.
15. Mahrholdt H, Wagner A, Judd RM, Sechtem U, Kim RJ. Delayed enhancement cardiovascular magnetic resonance assessment of non-ischaemic cardiomyopathies. *Eur Heart J.* 2005;26:1461-74.
16. Choudhury L, Mahrholdt H, Wagner A, Choi KM, Elliott MD, Klocke FJ, et al. Myocardial scarring in asymptomatic or mildly symptomatic patients with hypertrophic cardiomyopathy. *J Am Coll Cardiol.* 2002;40:2156-64.
17. McKee PA, Castelli WP, McNamara PM, Kannel WB. The natural history of congestive heart failure: the Framingham study. *N Engl J Med.* 1971;285:1441-6.
18. Klem I, Weinsaft JW, Bahnon TD, Hegland D, Kim HW, Hayes B, et al. Assessment of myocardial scarring improves risk stratification in patients evaluated for cardiac defibrillator implantation. *J Am Coll Cardiol.* 2012;60:408-20.
19. Kramer CM, Barkhausen J, Flamm SD, Kim RJ, Nagel E. Standardized cardiovascular magnetic resonance (CMR) protocols 2013 update. *J Cardiovasc Magn Reson.* 2013;15:91.
20. Sato T, Tsujino I, Ohira H, Oyama-Manabe N, Ito YM, Noguchi T, et al. Paradoxical interventricular septal motion as a major determinant of late gadolinium enhancement in ventricular insertion points in pulmonary hypertension. *PLoS One.* 2013;8:e66724.
21. Oyama-Manabe N, Ishimori N, Sugimori H, Van Cauteren M, Kudo K, Manabe O, et al. Identification and further differentiation of subendocardial and transmural myocardial infarction by fast strain-encoded (SENC) magnetic resonance imaging at 3.0 Tesla. *Eur Radiol.* 2011;21:2362-8.
22. Aikawa T, Oyama-Manabe N, Naya M, Ohira H, Sugimoto A, Tsujino I, et al. Delayed contrast-enhanced computed tomography in patients with known or suspected cardiac sarcoidosis: a feasibility study. *Eur Radiol.* 2017; doi: 10.1007/s00330-017-4824-x.
23. Schulz-Menger J, Bluemke DA, Bremerich J, Flamm SD, Fogel MA, Friedrich MG, et al. Standardized image interpretation and post processing in cardiovascular magnetic resonance: Society for Cardiovascular Magnetic Resonance (SCMR) board of trustees task force on standardized post processing. *J Cardiovasc Magn Reson.* 2013;15:35.
24. Werner RA, Maya Y, Rischpler C, Javadi MS, Fukushima K, Lapa C, et al. Sympathetic nerve damage and restoration after ischemia-reperfusion injury as assessed by <sup>11</sup>C-hydroxyephedrine. *Eur J Nucl Med Mol Imaging.* 2016;43:312-8.
25. Boogers MJ, Borleffs CJ, Henneman MM, van Bommel RJ, van Ramshorst J, Boersma E, et al. Cardiac sympathetic denervation assessed with <sup>123</sup>I-iodine metaiodobenzylguanidine imaging predicts ventricular arrhythmias in implantable cardioverter-defibrillator patients. *J Am Coll Cardiol.* 2010;55:2769-77.
26. Huikuri HV, Castellanos A, Myerburg RJ. Sudden death due to cardiac arrhythmias. *N Engl J Med.* 2001;345:1473-82.
27. Matsunari I, Schricke U, Bengel FM, Haase HU, Barthel P, Schmidt G, et al. Extent of cardiac sympathetic neuronal damage is determined by the area of ischemia in patients with acute coronary syndromes. *Circulation.*

2000;101:2579-85.

28. Mitrani RD, Klein LS, Miles WM, Hackett FK, Burt RW, Wellman HN, et al. Regional cardiac sympathetic denervation in patients with ventricular tachycardia in the absence of coronary artery disease. *J Am Coll Cardiol.* 1993;22:1344-53.

29. Akutsu Y, Kaneko K, Kodama Y, Li HL, Kawamura M, Asano T, et al. The significance of cardiac sympathetic nervous system abnormality in the long-term prognosis of patients with a history of ventricular tachyarrhythmia. *J Nucl Med.* 2009;50:61-7.

**Figure legends**

**Fig. 1** Representative images in patients with (a) and without (b) coronary artery disease. **a** A 65-year-old man with prior lateral myocardial infarction. Cine images show regional wall motion abnormality in the inferior to lateral wall. Late gadolinium enhancement (LGE) image shows subendocardial infarction (red arrows).  $^{11}\text{C}$ -hydroxyephedrine ( $^{11}\text{C}$ -HED) positron emission tomography (PET) shows reduced uptake (white arrows), which exceeds the extent of LGE. The polar map of  $^{11}\text{C}$ -HED retention index (RI) shows regional decrease in the inferior to lateral wall. **b** A 65-year-old man with hypertrophic cardiomyopathy. Cine images show asymmetric hypertrophy of the interventricular septum (end-diastolic wall thickness, 24 mm). LGE image shows midwall hyperenhancement in the interventricular septum, at the insertion points of the right ventricle (red arrows).  $^{11}\text{C}$ -HED PET and the polar map of  $^{11}\text{C}$ -HED RI shows regional decrease in the septal to inferior wall (white arrows)

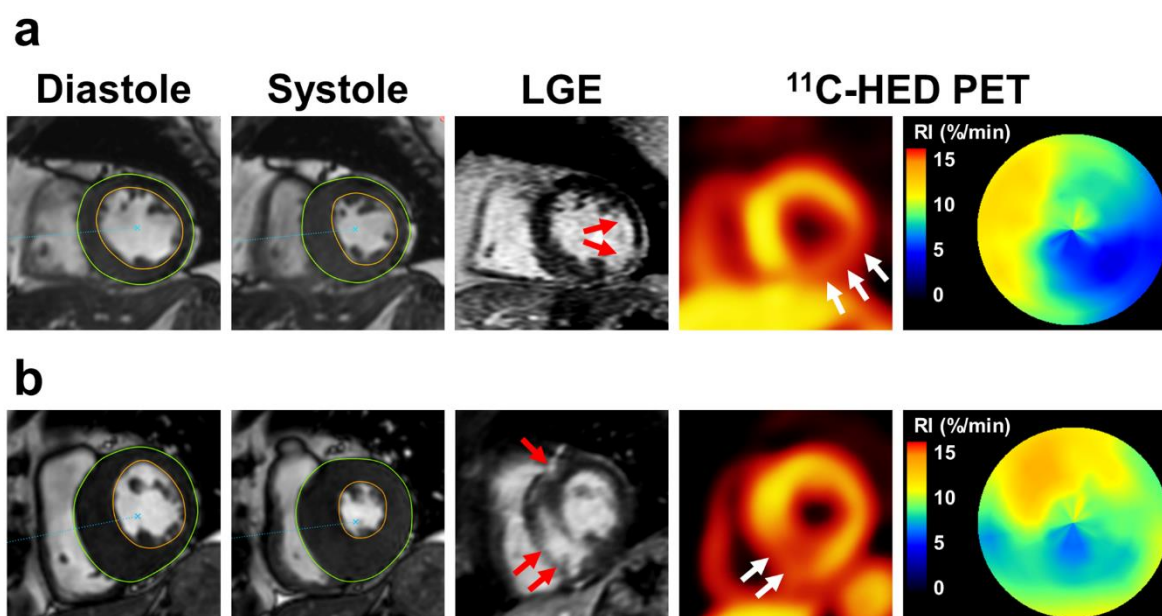
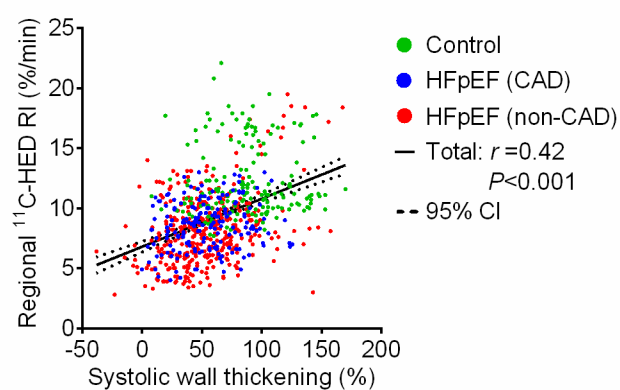
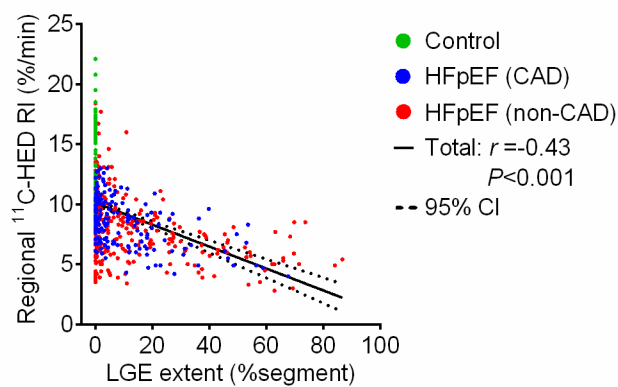


**Fig. 2** Scatter plots show the association between regional  $^{11}\text{C}$ -hydroxyephedrine ( $^{11}\text{C}$ -HED) retention index (RI) and systolic wall thickening (**a**), the extent of myocardial late gadolinium enhancement (LGE) (**b**), or left ventricular end-diastolic wall thickness (**c**) on a per-segment basis. HFpEF = heart failure with preserved ejection fraction, CAD = coronary artery disease, CI = confidence interval

**a**



**b**



**c**

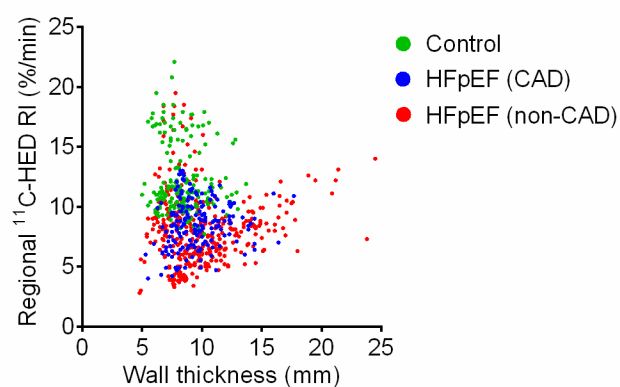
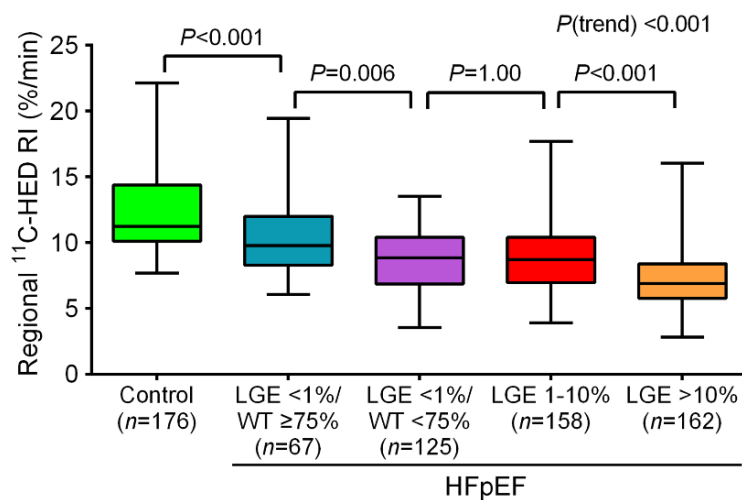


**Fig. 3 a** Box-and-whisker plots showing the distributions of regional  $^{11}\text{C}$ -hydroxyephedrine ( $^{11}\text{C}$ -HED) retention index (RI) in the control and patient groups categorized by systolic wall thickening (WT) and the extent of myocardial late gadolinium enhancement (LGE). The data show a modest stepwise decrease in regional  $^{11}\text{C}$ -HED RI with increasing LGE extent and decreasing WT. **b** Impaired regional  $^{11}\text{C}$ -HED RI (< 10%/min; the lower quartile value of the control group segments) was found in 76% of all segments in 32 patients with HFpEF (excluding the 2 patients with cardiac amyloidosis). The majority of segments with impaired regional  $^{11}\text{C}$ -HED RI had decreased systolic wall thickening and the presence of LGE. Numbers in parentheses are numbers of segments

**a**



**b**

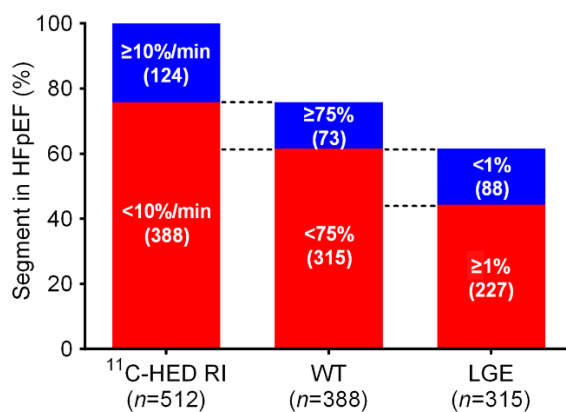


**Table 1**Clinical Characteristics of the Study Participants ( $n = 45$ )

| Characteristics                                   | Control<br>( $n = 11$ ) | HFpEF with CAD<br>( $n = 11$ ) | HFpEF without<br>CAD<br>( $n = 23$ ) | <i>P</i> -value |
|---|-------------------------|--------------------------------|--------------------------------------|-----------------|
| Age (y)   | 71 (50–72)              | 65 (57–76)                     | 64 (52–74)                           | 0.94            |
| Male/female                                       | 5/6                     | 11/0†                          | 12/11§                               | 0.012           |
| Body mass index (kg/m <sup>2</sup> )              | 22.5 (20.9–27.9)        | 23.7 (21.4–27.2)               | 22.3 (20.8–27.1)                     | 0.77            |
| NYHA functional class (I/II/III/IV)               | –                       | 1/8/2/0                        | 3/13/7/0                             | 0.69            |
| Hypertension                                      | 9 (82%)                 | 9 (82%)                        | 10 (43%)                             | 0.038           |
| Diabetes  | 0 (0%)                  | 5 (45%)†                       | 8 (35%)                              | 0.045           |
| Hyperlipidaemia                                   | 6 (55%)                 | 10 (91%)                       | 12 (52%)                             | 0.08            |
| Atrial fibrillation                               | 0 (0%)                  | 5 (45%)†                       | 6 (26%)                              | 0.048           |
| Prior myocardial infarction                       | 0 (0%)                  | 11 (100%)*                     | 0 (0%)‡                              | < 0.001         |
| Diagnosis of HFpEF, over 2 years ago              | –                       | 5 (45%)                        | 10 (43%)                             | 0.93            |
| Hospitalization for heart failure within 6 months | –                       | 5 (45%)                        | 6 (26%)                              | 0.28            |
| Blood data  |                         |                                |                                      |                 |
| B-type natriuretic peptide (pg/mL)                | 13.1<br>(8.3–19.9)      | 68.2<br>(20.2–211.0)†          | 81.8<br>(29.4–260.0)*                | 0.001           |
| Norepinephrine (pg/mL)                            | 429 (298–614)           | 366 (164–552)                  | 299 (243–390)                        | 0.32            |
| Troponin T (ng/mL)                                | 0.005<br>(0.003–0.010)  | 0.014<br>(0.010–0.037)†        | 0.024<br>(0.010–0.058)*              | < 0.001         |
| Medications                                       |                         |                                |                                      |                 |
| ACE-Is or ARBs                                    | 5 (45%)                 | 10 (91%)                       | 17 (74%)                             | 0.06            |
| β-blockers  | 1 (9%)                  | 10 (91%)*                      | 17 (74%)*                            | < 0.001         |
| Aldosterone antagonists                           | 1 (9%)                  | 3 (27%)                        | 2 (9%)                               | 0.30            |
| Diuretics   | 1 (9%)                  | 6 (55%)                        | 8 (35%)                              | 0.08            |
| Calcium-channel blockers                          | 7 (63%)                 | 4 (36%)                        | 8 (35%)                              | 0.26            |
| Statins   | 3 (27%)                 | 11 (100%)*                     | 8 (35%)‡                             | < 0.001         |
| Antiplatelet agents                               | 1 (9%)                  | 11 (100%)*                     | 2 (9%)‡                              | < 0.001         |
| Warfarin  | 0 (0%)                  | 3 (27%)                        | 2 (9%)                               | 0.12            |
| DOACs   | 0 (0%)                  | 2 (18%)                        | 5 (22%)                              | 0.03            |

\* $P < 0.01$  vs. control.† $P < 0.05$  vs. control.‡ $P < 0.01$  vs. HFpEF with CAD.§ $P < 0.05$  vs. HFpEF with CAD.

HFpEF = heart failure with preserved ejection fraction; CAD = coronary artery disease; NYHA = New York

Heart Association; ACE-Is = angiotensin-converting enzyme inhibitors; ARBs = angiotensin II receptor

blockers; DOACs = direct oral anticoagulants.

Data are expressed as median (interquartile range) or  $n$  (%).

**Table 2**

<sup>11</sup>C-hydroxyephedrine (<sup>11</sup>C-HED) Positron Emission Tomography and Cardiac Magnetic Resonance Imaging  
Results on a Per-Participant Basis

| Parameter                                 | Control<br>(n = 11) | HFpEF with CAD<br>(n = 11) | HFpEF without CAD<br>(n = 23) | P-value |
|---|---------------------|----------------------------|-------------------------------|---------|
| LV end-diastolic volume (mL)              | 77.4 (71.2–90.4)    | 117.2 (83.3–136.2)†        | 121.2 (94.0–152.1)*           | 0.002   |
| LV end-systolic volume (mL)               | 24.2 (15.4–26.4)    | 58.4 (41.8–66.5)*          | 58.2 (37.0–95.1)*             | < 0.001 |
| LV ejection fraction (%)                  | 70 (67–79)          | 51 (42–56)*                | 46 (36–59)*                   | < 0.001 |
| LV mass (g)                               | 80.7 (71.1–101.9)   | 112.2 (88.6–136.2)†        | 127.8 (102.3–139.7)*          | 0.003   |
| Mean LV end-diastolic wall thickness (mm) | 8.3 (6.9–9.9)       | 9.2 (8.2–11.2)             | 9.2 (8.1–11.9)                | 0.16    |
| Mean systolic wall thickening (%)         | 89.6 (73.5–96.1)    | 58.5 (44.9–61.5)*          | 52.0 (39.9–62.3)*             | < 0.001 |
| LGE extent (%LV)‡                         | 0 (0–0)             | 8.5 (3.8–13.4)*            | 4.8 (0.8–23.7)*               | < 0.001 |
| Global <sup>11</sup> C-HED RI (%/min)     | 11.1 (10.3–16.0)    | 8.5 (7.5–9.6)*             | 7.5 (6.1–9.5)*                | < 0.001 |
| <sup>11</sup> C-HED CVRI (%)              | 7.3 (6.4–9.5)       | 15.9 (10.5–24.6)*          | 16.4 (10.4–21.9)*             | < 0.001 |
| Denervation-scar mismatch (%LV)           | –                   | 6.3 (0–12.5)               | 0 (0–25.0)                    | 0.94    |

\* $P < 0.01$  vs. control.

† $P < 0.05$  vs. control.

‡Excluding the 2 patients with cardiac amyloidosis.

HFpEF = heart failure with preserved ejection fraction; CAD = coronary artery disease; LV = left ventricular;

LGE = late gadolinium enhancement; RI = retention index; CVRI = coefficient of variation of regional retention index among the 17 segments.

Data are expressed as median (interquartile range).

**Table 3**

Correlation Coefficient between Global  $^{11}\text{C}$ -hydroxyephedrine ( $^{11}\text{C}$ -HED) positron emission tomography and Cardiac Magnetic Resonance Imaging Parameters on a Per-Participant Basis

|  | LV ejection fraction (%) | LV end-diastolic volume (mL) | LV end-systolic volume (mL) | LV mass (g)        | LGE extent (%LV) <sup>‡</sup> |
|--|--------------------------|------------------------------|-----------------------------|--------------------|-------------------------------|
| Global $^{11}\text{C}$ -HED RI (%/min) | 0.53*                    | -0.37 <sup>†</sup>           | -0.50*                      | -0.32 <sup>†</sup> | -0.49*                        |
| $^{11}\text{C}$ -HED CVRI (%)          | -0.51*                   | 0.44*                        | 0.50*                       | 0.30 <sup>†</sup>  | 0.73*                         |

\* $P < 0.01$

<sup>†</sup> $P < 0.05$

<sup>‡</sup>Excluding the 2 patients with cardiac amyloidosis.

LV = left ventricular; LGE = late gadolinium enhancement; RI = retention index; CVRI = coefficient of variation of regional retention index among the 17 segments.

**Table 4**

Predictors of Regional Sympathetic Innervation in Patients with Heart Failure with Preserved Left Ventricular Ejection Fraction (32 patients, 512 segments)\*

| Variable   | $\beta$ | SE   | 95% CI         | <i>P</i> -value |
|--|---------|------|----------------|-----------------|
| Systolic wall thickening (per 10%)                 | 0.06    | 0.02 | 0.02 to 0.10   | 0.001           |
| LGE extent (per 10% of segment)                    | -0.21   | 0.03 | -0.27 to -0.15 | < 0.001         |
| Left ventricular end-diastolic wall thickness (mm) | 0.15    | 0.03 | 0.09 to 0.20   | < 0.001         |

\*Mixed-effects model adjusting for age, sex, body mass index, past medical history (hypertension, diabetes, hyperlipidaemia, and atrial fibrillation), the presence of coronary artery disease,  $\beta$ -blockers use, and intermediate left ventricular ejection fraction (< 50%).

SE = standard error; CI = confidence interval; LGE = late gadolinium enhancement.